Bilayer Splitting in the Electronic Structure of Heavily Overdoped $Bi_2Sr_2CaCu_2O_{8+\delta}$

D. L. Feng, N. P. Armitage, D. H. Lu, A. Damascelli, J. P. Hu, P. Bogdanov, A. Lanzara, F. Ronning, K. M. Shen, H. Eisaki, C. Kim, and Z.-X. Shen

Department of Physics, Applied Physics and Stanford Synchrotron Radiation Laboratory, Stanford University, Stanford, California 94305

J.-i. Shimoyama and K. Kishio

Department of Applied Chemistry, University of Tokyo, Tokyo, 113-8656, Japan

(Received 18 January 2001)

The electronic structure of heavily overdoped $Bi_2Sr_2CaCu_2O_{8+\delta}$ is investigated by angle-resolved photoemission spectroscopy. The long-sought bilayer band splitting in this two-plane system is observed in both normal and superconducting states, which qualitatively agrees with the bilayer Hubbard model calculations. The maximum bilayer energy splitting is about 88 meV for the normal state feature, while it is only about 20 meV for the superconducting peak.

DOI: 10.1103/PhysRevLett.86.5550 PACS numbers: 71.18.+y, 74.72.Hs, 79.60.Bm

High temperature superconductors (HTSC's), as doped Mott insulators, show strong doping dependent behavior. The underdoped regime of the HTSC's is characterized by its unconventional properties, such as the pseudogap and non-Fermi liquid transport behavior. On the other hand, the overdoped regime is considered to be more "normal," partly because of the absence of a pseudogap and more Fermi-liquid–like behavior. It is very challenging and important for HTSC theories to be able to explain the phenomenology in both regimes. Angle-resolved photoemission spectroscopy (ARPES), one of the most direct probes of the electronic structure, has contributed greatly to the understanding of the electronic structure of the HTSC's [1]. However, most systems studied by ARPES have either low T_c's [below 40 K for $La_{2-x}Sr_xCuO_{4+\delta}$ (LSCO), and $Bi_2Sr_2CuO_{6+\delta}$ (Bi2201)], or doping limitations [only up to slightly overdoping for $Bi_2Sr_2CaCu_2O_{8+\delta}$ (Bi2212) and $YBa_2Cu_3O_{7-y}$ (YBCO)]. For a complete understanding, it is very important to study the heavily overdoped systems, especially Bi2212, which is the most studied system by ARPES.

Recent advances in high pressure annealing techniques have made it possible to synthesize heavily overdoped Bi2212. In this paper, we report ARPES measurements of the electronic structure of heavily overdoped Bi2212. We show that the long-sought bilayer band splitting (BBS) exists for both normal and superconducting states of this material over a large fraction of the Brillouin zone. The detection of BBS, which has been predicted by various calculations [2–6], but not observed in earlier ARPES data [7], enables us to address several important issues. First, it provides a very detailed test for the theoretical calculations, with our experimental results favoring the bilayer Hubbard model [6] over LDA calculations [2,4]. Second, it shows the novel result that the bilayer splitting energy in the superconducting state is only about 23% of the normal state splitting. Third, it provides an explanation for the detection of a "peak-dip-hump" structure in the normal state of heavily overdoped samples [8,9].

Heavily overdoped Bi2212 samples [T_C(onset) = 65 K, $\Delta T_C(10\% \sim 90\%) = 3$ K, denoted as OD65] were synthesized by annealing floating-zone-grown single crystals under oxygen pressure $P_{O_2} = 300$ atm at 300 °C for two weeks, and characterized by various techniques. Magnetic susceptibility measurements (inset of Fig. 1) do not show the presence of a second phase. Laue diffraction and low energy electron diffraction (LEED) patterns show that its superstructure and surface resemble those of optimally doped samples, and the flatness of the cleaved sample surface is confirmed by the small laser reflection from the sample. Angle-resolved photoemission experiments were performed at beam line V-4 of Stanford Synchrotron Radiation Laboratory (SSRL) with a Scienta SES200 electron analyzer, which can take spectra in a narrow cut of $0.5° \times 14°$ simultaneously in its angular mode with an angular resolution as good as 0.12° along the cut direction. The data were collected with polarized synchrotron light from a normal incidence monochromator, where the intensity of the second order light is extremely weak, as well as nonmonochromatic and unpolarized He-Iα light. The intensity of other lines is fairly weak, which contributes a smooth background to the spectra in the interested range and does not affect the conclusions drawn below. The overall energy resolution is about 10 meV. Samples were aligned by Laue diffraction, and cleaved *in situ* at a pressure better than 5×10^{-11} torr (1.3×10^{-10} torr with He lamp turned on). Sample aging effects are negligible during the measurement.

A typical Fermi surface (FS) sketch of the Bi2212 system without considering the bilayer band splitting is shown in Fig. 1 [7]. One can see the main FS, its superstructure images due to structure modulations in the BiO layer, which are typically about $(0.21\pi, 0.21\pi)$ away from the main FS, and the shadow band FS, which is a (π, π)

 0031-9007/01/86(24)/5550(4)$15.00

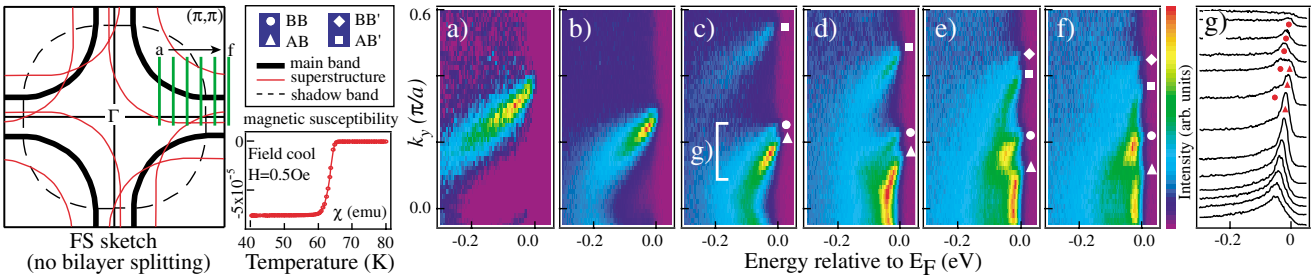

FIG. 1 (color). (a)–(f) False color plot of the OD65 normal state ($T = 75$ K) ARPES spectra taken with 22.7 eV synchrotron light. Features AB, BB, and their superstructure images AB′ and BB′ are indicated by triangles, circles, squares, and diamonds, respectively. The EDC's near the Fermi crossing in (c) (indicated by "[") are plotted in (g). The angular resolution is 0.3°.

foldback of the main FS [10], and is very weak at 22 eV photon energy due to matrix element effects [7]. Photoemission intensity taken in the normal state of OD65 along the momentum cuts indicated by the green lines in the FS sketch are shown in Figs. 1(a)–1(f) as a function of momentum and binding energy. In this way, one can clearly see the centroids of the dispersing features. For example, Fig. 1(a) shows that one band disperses and crosses the Fermi energy along a momentum cut that goes through the d-wave node region. Away from the nodal region, this seemingly single feature splits evidently into two features, features AB and BB, starting from Fig. 1(c). The photoemission intensities in the bracketed region are replotted in the form of energy distribution curves (EDC's) in Fig. 1(g), where one can see two peaks cross the Fermi level about 0.9° apart. This splitting increases when approaching the $(\pi, 0)$ region. In Fig. 1(f), features AB and BB are well separated, and two more weaker features (AB′ and BB′) are clearly visible as well; these are the superstructure images of features AB and BB. The absence of splitting in the nodal region is checked with the best achievable angular resolution (~0.12°).

The observed Fermi crossings in Figs. 1(c)–1(f) deviate from what is expected from the FS sketch shown in Fig. 1, but can be naturally interpreted by the presence of BBS. Because the Bi2212 ARPES features are considered to be mainly contributed by the antibonding $x^2 - y^2$ state in the CuO_2 plane, and Bi2212 has two CuO_2 planes per unit cell, the intrabilayer coupling would cause a splitting. As we will see later, the observed splitting agrees with what is expected from a bilayer system [6]. This interpretation is also supported by recent studies of heavily overdoped single-layer Bi2201, where only one band was observed [11]. Since feature AB is always at lower binding energy than feature BB at a given momentum, we assign the antibonding band (AB) to feature AB, and bonding band (BB) to feature BB.

The Fermi surfaces can be determined by determining Fermi crossings of the bands (dispersion method), or determining the local maxima of the low energy ARPES spectral weight distribution (spectral weight method) (Fig. 2) [12]. One can see two main FS's, one for AB and the other for BB, and their corresponding superstructure images (AB′ and BB′). The observed holelike Fermi surface topology is consistent with early findings in less overdoped Bi2212 systems at similar photon energies. These FS's overlap in the nodal region and gradually depart from each other when approaching the $(\pi, 0)$ region. Figure 2(b) shows EDC's along one cut that crosses all of the four Fermi surfaces. At 22.7 eV photon energy [lower right half of Fig. 2(a)], the AB has more weight near E_F than the BB, and this situation is reversed at 20 eV [upper left half of Fig. 2(a)]. This strong photon energy dependence of the relative intensities of the AB and BB is consistent with the BBS, because the AB and BB have odd and even symmetries, respectively, along the c axis. By tuning the incident photon energy, the wave vector of the final electron state along the c axis is changed, which changes the photoemission cross sections between the final state and the initial BB and AB differently due to their opposite symmetries. The fact that we see BBS all over the FS and in the superstructure images (AB′ and BB′) away from the $(\pi, 0)$ region rules out the possibility that the split FS's are artifacts caused by the superstructure. Moreover, because the intensity of BB is weaker than that of AB in the 22.7 eV photon energy data, AB cannot be a superstructure

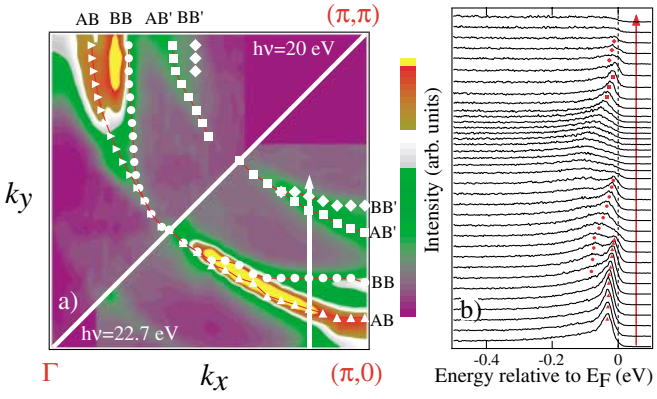

FIG. 2 (color). (a) False color plot of the spectral weight mapping near E_F ([−20 meV, 10 meV]) of OD65 taken at 22.7 eV (lower right half, $T = 75$ K) and 20 eV (upper left half, $T = 80$ K) (note they are from different experiments). The Fermi surface determined by dispersion is also plotted for antibonding states (AB, triangles), bonding states (BB, circles), superstructure images of antibonding states (AB′, squares), and bonding states (BB′, diamonds). (b) ARPES spectra along the cut indicated by the arrow in (a).

of BB, and vice versa for the data taken at 20 eV photon energy.

To understand the effect of the BBS on the superconducting state, spectra were taken in both the normal and superconducting states near the $(0, \pi)$ region (Fig. 3), where the splitting is greatest. It was found that in this region, the ARPES line shape of Bi2212 evolves dramatically across T_c from a broad spectrum in the normal state into a well-known peak-dip-hump (PDH) structure in the superconducting state [13].

In the normal state [Fig. 3(a)], the antibonding state crosses E_F near n4 and n-4, while the bonding state disperses through the Fermi energy around spectra n8 and n-8. The presence of two features in the normal state was reported earlier [8,9], and suggested to be an anomalous normal state counterpart to the conventional superconducting PDH [8]. Here, we show that this feature is actually due to the bilayer splitting. In spectra n-3 through n2, the BB is at high binding energy and thus broad, while the AB is at low binding energy and thus sharp, which conspire to give a PDH-like structure. We stress that this is different from the PDH structure that turns on at T_c.

In the superconducting state [Fig. 3(b)], the low energy part of the spectra evolves into two sharp superconducting peaks. It appears that both the normal state BB and AB develop their own superconducting PDH structure. BB hump is observed near the normal state BB binding energy, whereas AB hump is buried under the superconducting peaks, which presumably locates also near the normal state AB binding energy. Similar to the superconducting peak reported before in less overdoped samples, both BB and AB superconducting peaks lose their intensity upon crossing the corresponding normal state BB/AB FS's. More specifically, spectra s7 and n7 [replotted in Fig. 3(c)], which consist mainly of the BB, strongly resemble the normal and superconducting state spectra from overdoped samples with less carrier doping [14]. When the BB superconducting peak disperses to higher binding energies, it becomes weaker and presumably contributes very little to the sharp peak seen at s0. Therefore, the observed sharp peak at s0 can be regarded as being mainly due to the antibonding state. For spectra containing two peaks, they can be fitted by two PDH's, as shown in Fig. 3(c) for s4.

The dispersions extracted from Fig. 3 are summarized in Fig. 4(a). Because the superconducting peak intensity of the BB is very weak near $(\pi, 0)$, its position is extrapolated and shown as the dotted line. Although the BB and AB superconducting peaks have different dispersions, their minimum binding energies near their respective FS's are almost the same ($\sim$16 meV), which shows that the BB and AB have the same d-wave superconducting gap amplitude. The maximum energy splittings can be extracted from the binding energies at $(\pi, 0)$. They are found to be about 88 meV for the normal state bands, and interestingly, only about 20 meV for the superconducting peaks. The striking difference in the splitting energies cannot be explained with conventional theories, where quasiparticles below T_c have an energy of $E_{\mathbf{k}} = \sqrt{\Delta_{\mathbf{k}}^2 + \varepsilon_{\mathbf{k}}^2}$, with $\varepsilon_{\mathbf{k}}$ and $\Delta_{\mathbf{k}}$ being the normal state quasiparticle energy and superconducting gap, respectively. The small splitting energy of the superconducting peak also counters the naive expectation that global phase coherence below T_c will enhance the c-axis

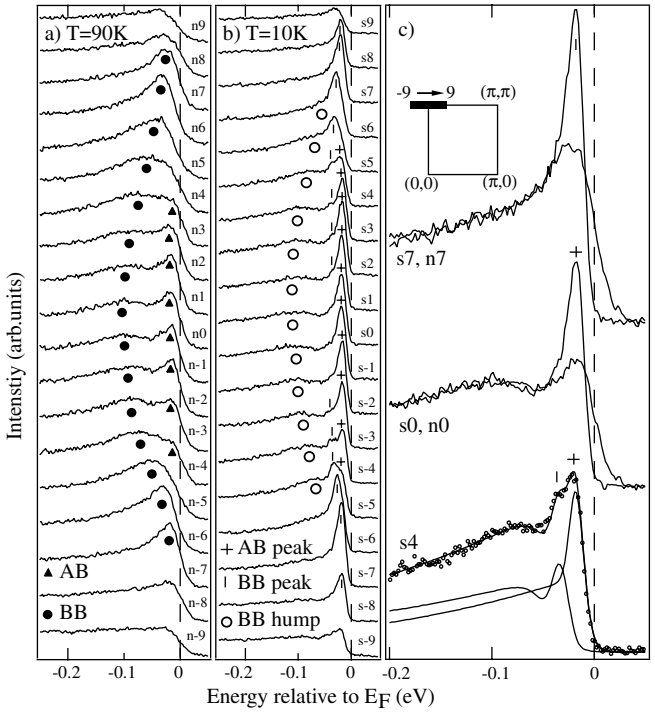

FIG. 3. ARPES spectra taken on OD65 with He-Iα light for (a) normal state, and (b) superconducting state. The angular resolution is 0.56°. (c) shows selected spectra from (a) and (b). Note that the fit of s4 is not unique. The spectra are taken along $(-0.24\pi, \pi) - (0.24\pi, \pi)$, and labeled from -9 to 9 as shown in the inset of (c).

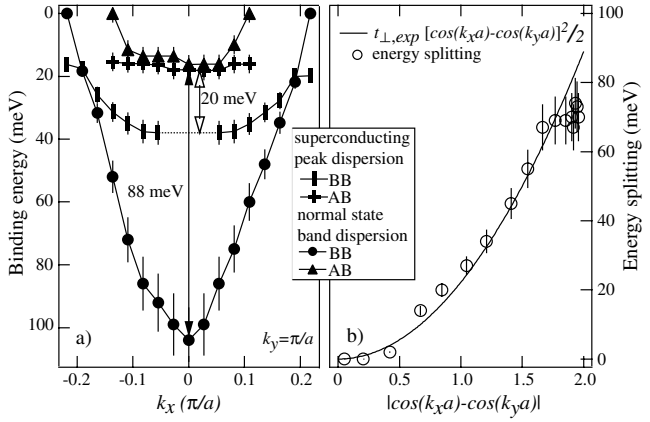

FIG. 4. (a) Dispersion extracted from Fig. 3. (b) Energy splitting along the AB Fermi surface, which are obtained from data shown in Fig. 1. It is simply the binding energy of the BB, since the binding energy of AB is zero at its Fermi surface. The curve is $t_{\perp,\mathrm{exp}}[\cos(k_x a) - \cos(k_y a)]^2/2$, where $t_{\perp,\mathrm{exp}} = 44 \pm 5$ meV. Error bars are due to the uncertainties in determining the energy position.

coupling and thus cause larger splitting. Instead, the data suggest that the superconducting peak is a new quasiparticle generated upon the superconducting phase transition. This is in agreement with the earlier observation that the weight of the superconducting peak is closely related to the carrier doping level and the condensation fraction of the system [14]. We hope the new data can stimulate more theoretical works on this issue.

The nature of the normal state BBS as a function of momentum and energy puts strong constraints on theoretical models. A maximum momentum splitting near $(\pi, 0)$ contradicts early LDA calculations, where the calculated BiO Fermi surface near $(\pi, 0)$ causes a very small splitting of the CuO_2 bands near $(\pi, 0)$ [2]. However, it does agree qualitatively with bilayer LDA calculations that consider only bands from the two CuO_2 planes [4], and the bilayer Hubbard model, which is based on the bilayer LDA band calculations plus additional on-site Coulomb repulsion [6]. The bilayer Hubbard model predicts two AB/BB Fermi surfaces similar to the data for similar carrier doping levels [6].

The bilayer LDA calculations [4] predicted the normal state bilayer energy splitting to be $2t_\perp(\mathbf{k}) = t_\perp[\cos(k_x a) - \cos(k_y a)]^2/2$, where $t_\perp(\mathbf{k})$ is the anisotropic intrabilayer hopping. It indicates that the maximum energy splitting is $2t_\perp$ at $(\pi, 0)$. This agrees with the data, and one obtains the experimental intrabilayer hopping $t_{\perp,\mathrm{exp}} = 44 \pm 5$ meV. To test this over a large momentum range, the normal state energy splitting along the AB Fermi surface [Fig. 4(b)] were extracted from the data in Figs. 1 and 2. Indeed, the data can be fitted very well by $t_{\perp,\mathrm{exp}}[\cos(k_x a) - \cos(k_y a)]^2/2$, but quantitatively, the experimental maximum energy splitting of 88 meV $(2t_{\perp,\mathrm{exp}})$, is much smaller than the 300 meV $(2t_{\perp,\mathrm{LDA}})$ splitting predicted by the bilayer LDA calculations [4]. On the other hand, the data agree better with the bilayer Hubbard model [6], which predicted a similar anisotropic energy splitting with 40 meV maximum energy splitting at $(\pi, 0)$ for the similar doping level. This is because unlike the bilayer LDA calculations, the bilayer Hubbard model considers strong correlations, and strong on-site Coulomb repulsion (or correlations) will substantially reduce the hopping to an occupied site thus reducing the effective intrabilayer hopping [5]. Based on this, its small splitting energy scale (40 meV) may suggest that weaker on-site Coulomb repulsion should be adopted in the bilayer Hubbard model (at least for the heavily overdoped case). We note that $t_{\perp,\mathrm{exp}}$ is of similar magnitude of the gap, and is a significant fraction of the in-plane exchange coupling J, and the bandwidth. Therefore, the intrabilayer coupling should be considered in models describing Bi2212.

A natural question is why the bilayer band splitting is particularly prominent in heavily overdoped materials. This is mainly because the more Fermi-liquid–like behavior in the heavily overdoped regime results in much better defined quasiparticles, i.e., much sharper features. The absence of two well-defined features in the spectra of less overdoped samples does not necessarily imply the absence of the BBS. In fact, with improved resolution, preliminary studies have found signatures of BBS in the normal state of slightly overdoped Bi2212 samples [15].

In summary, the bilayer band splitting in the heavily overdoped Bi2212 system is observed in both normal and superconducting states by ARPES measurements, which qualitatively agrees with the bilayer Hubbard model calculations. The different energy splitting scales reported here provide new information for the behavior of the superconducting peak, which cannot be well understood in the current theoretical framework and needs further investigation.

SSRL is operated by the DOE Office of Basic Energy Science Divisions of Chemical Sciences and Material Sciences. The Material Sciences Division also provided support for the work. The Stanford experiments are also supported by NSF Grant No. 9705210 and ONR Grant No. N00014-98-1-0195-A00002. D. L. F. and Z. X. S. want to thank S. Maekawa, B. O. Wells, Z. Yusof, Y. Lu, D. S. Dessau, and S. Chakravarty for helpful discussions.

[1] D. W. Lynch and C. G. Olson, *Photoemission Studies of High-Temperature Superconductors* (Cambridge University Press, Cambridge, 1999); Z.-X. Shen and D. S. Dessau, Phys. Rep. **253**, 2 (1995).
[2] S. Massidda *et al.,* Physica (Amsterdam) **152C**, 251 (1988); W. E. Pickett, Rev. Mod. Phys. **61**, 251 (1989).
[3] S. Chakravarty *et al.,* Science **261**, 337 (1993).
[4] O. K. Anderson *et al.,* J. Phys. Chem. Solids **12**, 1573 (1995).
[5] R. Eder *et al.,* Phys. Rev. B **51**, 3265 (1995).
[6] A. I. Liechtenstein *et al.,* Phys. Rev. B **54**, 12 505 (1996).
[7] H. Ding *et al.,* Phys. Rev. Lett. **76**, 1533 (1996).
[8] S. Rast *et al.,* Europhys. Lett. **51**, 103 (2000). An abrupt change in the measured ARPES spectra at a new temperature scale $T^+ \approx 85$ K is also reported. However, it is not observed in our experiments.
[9] Z. Yusof and B. O. Wells (private communication).
[10] P. Aebi *et al.,* Phys. Rev. Lett. **72**, 2757 (1994).
[11] D. L. Feng *et al.* (unpublished).
[12] We note that at 20 eV photon energy, the FSs determined by the dispersion method do not agree with those determined by the spectral weight method. The latter is affected by the photoemission matrix elements: when two features are very close and have similar intensities, the positions of the local spectral weight maxima shift due to the overlapping. However, the combination of both methods can give a qualitative and objective measurement of the FS.
[13] D. S. Dessau *et al.,* Phys. Rev. Lett. **66**, 2160 (1991).
[14] D. L. Feng *et al.,* Science **289**, 277 (2000); H. Ding *et al.,* cond-mat/0006143.
[15] P. Bogdanov, A. Lanzara, and Z.-X. Shen (unpublished); Y.-D. Chung, A. Gromko, and D. Dessau, cond-mat/0102386.